Beam-Surface Scattering Studies of the Individual and Combined Effects of VUV Radiation and Hyperthermal O, O_2, or Ar on FEP Teflon Surfaces

Amy L. Brunsvold, Jianming Zhang, Hari P. Upadhyaya, and Timothy K. Minton*

Department of Chemistry and Biochemistry, Montana State University, Bozeman, Montana 59717

ABSTRACT Beam-surface scattering experiments were used to probe products that scattered from FEP Teflon surfaces during bombardment by various combinations of atomic and molecular oxygen, Ar atoms, and vacuum ultraviolet (VUV) light. A laser-breakdown source was used to create hyperthermal (translational energies in the range 4−13 eV) beams of argon and atomic/molecular oxygen. The average incidence energy of these beams was tunable and was controlled precisely with a synchronized chopper wheel. A filtered deuterium lamp provided a source of VUV light in a narrow-wavelength range centered at 161 nm. Volatile products that exited the surfaces were monitored with a rotatable mass spectrometer detector. Hyperthermal O atoms with average translational energies above ~4 eV may react directly with a pristine FEP Teflon surface, and the reactivity appears to increase with the translational energy of the incident O atoms. VUV light or highly energetic collisions of O_2 or Ar may break chemical bonds and lead to the ejection of volatile products; the ejection of volatile products is enhanced when the surface is subjected to VUV light and energetic collisions simultaneously. Exposure to VUV light or to hyperthermal O_2 or Ar may increase the reactivity of an FEP Teflon surface to O atoms.

KEYWORDS: atomic oxygen • FEP Teflon • beam-surface scattering • VUV photodegradation • collision-induced dissociation • space environmental effects • synergistic effects

1. INTRODUCTION

Surfaces of spacecraft traveling in low Earth orbit (LEO) are exposed to an environment containing atomic oxygen, molecular nitrogen, electromagnetic radiation, ions, electrons, and high-energy charged particles. Atomic oxygen and molecular nitrogen are the major constituents in the residual atmosphere at LEO altitudes (1, 2), and they collide with spacecraft surfaces at relative velocities of ~7.4 km s^{-1} (3). These high relative velocities lead to gas−surface collisions with many electron volts of collision energy in the center-of-mass (c.m.) reference frame (4, 5). The energy associated with these hyperthermal collisions is in excess of many bond dissociation energies and may help promote materials degradation by allowing barriers to reaction or to collision-induced dissociation (CID) to be overcome. High fluxes of solar vacuum ultraviolet (VUV) radiation might contribute to the degradation of materials through various photochemical mechanisms. The VUV spectrum comprises radiation with wavelengths that span 100−200 nm, including the Lyman α line of atomic hydrogen (121 nm) (6). Fluorinated ethylene propylene (FEP) Teflon is commonly used as a thermal control material on space vehicles to provide protection from solar heating (7). However, FEP Teflon degrades upon exposure to the LEO environment. Various NASA missions, including the Long Duration Exposure Facility (LDEF) and the Hubble Space Telescope, have shown evidence of severe FEP Teflon degradation, including surface erosion, after exposure in LEO (8−14). Scanning electron microscope images obtained from the surfaces of FEP Teflon samples exposed to the LEO environment on the leading and trailing edges of the LDEF satellite showed different surface morphologies, suggesting different degradation mechanisms in the different environments (14). Although it is clear that the degradation mechanisms of FEP Teflon in LEO depend on the details of the environment, the dominant mechanisms by which FEP Teflon degrades in LEO have been the subject of much debate.

Many explanations have been proposed to account for the erosion and deterioration of the mechanical properties of FEP Teflon in LEO. It has been suggested that the erosion rate of FEP Teflon is enhanced synergistically under the combined exposure of VUV light and atomic oxygen, while the erosion rate by atomic oxygen alone is very low (15−18). However, Tagawa and co-workers (19, 20) found no synergistic effect in their study, in which they observed that the simultaneous exposure of a fluorocarbon polymer to a hyperthermal O-atom beam and to 172 nm VUV radiation produced mass loss that was the sum of the mass loss caused by the O-atom beam plus the mass loss caused by the VUV radiation. Their conclusion was thus that the mass loss was an additive, not a synergistic, effect. Skurat et al. (21) have suggested that it is only VUV light that is responsible for FEP Teflon degradation in LEO, and they have proposed a mechanism whereby VUV radiation breaks C−C bonds until smaller fragments of the chain are formed and become

* To whom correspondence should be addressed. Tel: 406-994-5394. Fax: 406-994-6011. E-mail: tminton@montana.edu.
Received for review August 21, 2008 and accepted August 27, 2008
DOI: 10.1021/am800015k

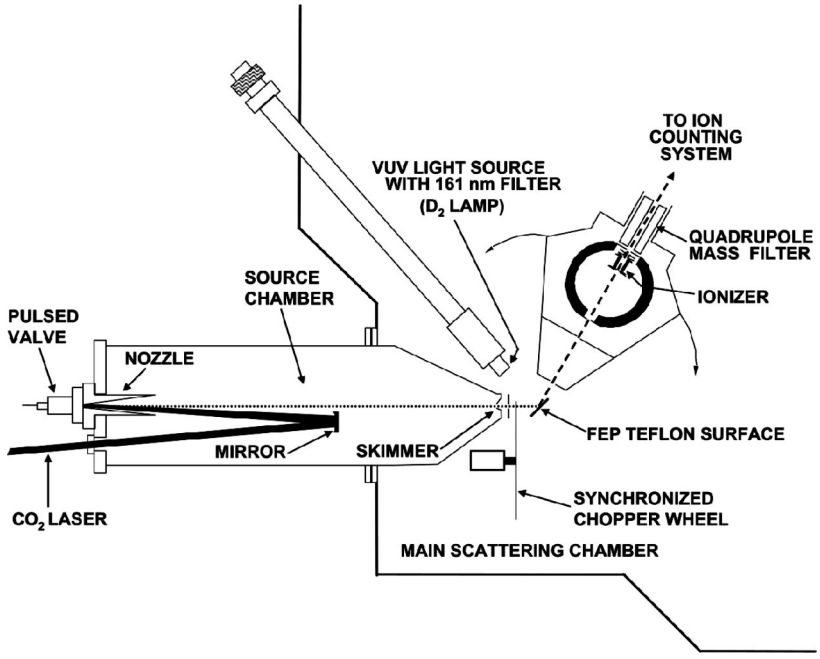

FIGURE 1. Schematic diagram of the crossed-molecular-beams apparatus, configured for gas−surface scattering experiments, showing the hyperthermal beam source, the target surface, the deuterium lamp, and the rotatable mass spectrometer detector.

volatile, thereby carrying mass away. Gindulyte et al. (22) discounted the role of VUV radiation altogether by proposing, based on calculated barriers of 2.9−3.3 eV for $O(^3P)$ reactions with small perfluorocarbon molecules that break a C−C bond (the calculated barrier was between 3.5 and 4.1 eV in the case of the smallest perfluorocarbon studied, C_2F_6), that collisions of $O(^3P)$ atoms with perfluorocarbons in LEO have enough energy to promote a direct reaction and may therefore lead to erosion of a fluorocarbon polymer surface regardless of the amount of VUV exposure. Troya and Schatz (23) added additional insight to the conclusions of Gindulyte et al. with their theoretical study of $O(^3P)$ reactions with small hydrocarbon (CH_4 and C_2H_6) and perfluorocarbon (CF_4 and C_2F_6) molecules. For $O(^3P) + C_2F_6$, they found that the lowest-energy transition state for C−C bond breaking was 2.52 eV above the reactants, which is lower in energy than the transition state reported by Gindulyte et al. However, more importantly, through their molecular dynamics calculations, they discovered that the C−C bond-breaking cross sections for the reaction of $O(^3P)$ with C_2F_6 remain negligibly small up to c.m. collision energies of ∼4.5 eV. A more recent study by Troya and co-workers on $Ar + C_2F_6$ collisions suggests that CID of the perfluorocarbon molecule might be more likely than an O-atom reaction as the collision energy climbs above 5 eV (24). Their results showed that C_2F_6 absorbs more energy in hyperthermal collisions than does its hydrocarbon analogue, C_2H_6. Thus, for collisions of a given energy, C_2F_6 is more susceptible to CID than C_2H_6. These theoretical results are consistent with preliminary crossed-beams studies in our laboratory on the gas-phase interactions of $O(^3P)$ and Ar with C_3F_8. For $O(^3P) + C_3F_8$ at a c.m. collision energy of ∼4.4 eV, we observed no evidence of O-containing products. When the collision energy involving O atoms was increased above 5 eV, we observed fragments that indicated that the C_3F_8 had been dissociated by the hyperthermal collisions, but the CID might have resulted from collisions with the O_2 component in the beam, which would have collision energies greater than 8 eV. Indeed, when Ar collided with C_3F_8 at ∼7 eV and higher, we also observed fragments that were indicative of CID. In contrast, we have not observed evidence of CID in crossed-beams studies of O or Ar collisions with the analogous hydrocarbon, C_3H_8. Although several studies have focused on the role of VUV light and its possible synergistic effects with atomic oxygen in the erosion of FEP Teflon (see, for example, refs 7, 14,−21, and 25−29), CID might also be important in the degradation of fluorocarbon polymers.

In order to improve our understanding of the erosion mechanisms of FEP Teflon in a LEO environment, we have conducted beam-surface scattering experiments that probed products scattered from an FEP Teflon surface when it was bombarded by various combinations of hyperthermal O atoms, O_2 molecules, and Ar atoms, as well as VUV light. The use of Ar to study hyperthermal collisions with FEP Teflon provided a model system that restricted the possible interactions to collisional processes only. These beam-surface scattering experiments were designed to probe the individual and combined effects of hyperthermal atomic oxygen, VUV radiation, and CID on the surfaces of FEP Teflon.

2. EXPERIMENTAL DETAILS

The experiments were conducted with the use of a crossed-molecular-beams apparatus, configured for gas−surface interactions (4, 30−32). A schematic diagram of the apparatus is shown in Figure 1. A laser-breakdown source based on an earlier design (33) was used to create pulsed, hyperthermal beams containing either Ar or a mixture of O and O_2 that were directed at an FEP Teflon sample surface. A rotatable mass spectrometer detector was used to identify volatile products that scattered from the surface as a function of the translational

energy of the incident Ar, O, or O_2. Volatile products were also detected when VUV light continuously irradiated an FEP Teflon surface. Finally, volatile products that emerged from the FEP Teflon surface were monitored, while a hyperthermal beam containing Ar or a mixture of O and O_2 was directed onto a surface that was simultaneously irradiated with VUV light. The number densities of all products that scattered into the mass spectrometer detector at a particular mass-to-charge ratio, m/z, were detected as a function of their arrival time, t, at the electron-bombardment ionizer (33.6 cm from the sample surface). The resulting number density distributions, $N(t)$, are commonly referred to as time-of-flight (TOF) distributions. "Time zero" in these distributions is typically the time at which the maximum flux of the incident beam pulse strikes the surface. In the case where the surface was continuously bombarded by VUV light with no additional bombardment by atoms or molecules, a spinning slotted disk ("chopper wheel") was placed between the sample and detector in order to modulate the signal. Each number density (or TOF) distribution was integrated according to $\sum N(t)/t$ in order to obtain the relative flux of species scattered into the detector at a given angle (34).

2.1. Preparation of an FEP Teflon Sample. One side of a 1-in.-diameter FEP Teflon sample was chemically altered with a surface etchant (Tetraetch) and bonded to a 1-in.-diameter silicon substrate with a thermally conductive, silver-filled adhesive (Ablebond 70-1). The adhesive was cured in air starting with 1 h at 323 K and then ramped to 473 K in three 50 K steps, with 1 h at each step. When mounted on the sample manipulator, the entire backside of the silicon substrate was in contact with metal surfaces that were heated by a resistive heater. Thermal conductivity to the entire sample was thus achieved, and thermal equilibrium between the FEP Teflon sample and the manipulator, whose temperature was measured with a thermocouple, ensured that the surface temperature was known. Before mounting on the sample manipulator, the sample surfaces were rinsed with a mixture of ultrapure trichloroethylene and ethanol (75% and 25% by volume, respectively). After an initial overnight bakeout, in vacuum, of the prepared sample at 373 K, the temperature of the sample was reduced and held at 343 K throughout the experiment. It was found that the bakeout was required to reduce outgassing of the volatile components of the sample to a negligible level.

2.2. VUV Light Irradiation. A 30 W deuterium lamp (Hamamatsu model L7292) provided continuous VUV radiation mainly in the wavelength range of 115–200 nm. Such a deuterium lamp has been used extensively to simulate the effects of solar VUV light on materials in the LEO environment (35). The orientation of the deuterium lamp in the apparatus may be seen in Figure 1. During the investigation of the effects of VUV irradiation alone on the surface of FEP Teflon, the lamp was used without filtering and the distance between the center of the lamp and the sample was 15 cm. With the lamp at this distance, the sample surface experienced ~90 times the equivalent solar irradiance in LEO (i.e., ~90 "suns") in the wavelength range 115–200 nm (36). The sample was irradiated with continuous VUV radiation, and TOF distributions of the products that emerged from the surface were detected at a variety of C_mF_n fragment mass-to-charge ratios with the mass spectrometer. For the experiments where beam-surface scattering was conducted in addition to VUV light exposure, a filter was used to narrow the wavelength range of the light falling on the sample. The band-pass filter had a transmission peak at 161 ± 2.5 nm, with a full width at half-maximum of 20 nm, and it transmitted ~12% of the irradiance of the deuterium lamp in this wavelength range. When filtered, the lamp was placed 12.7 cm from the sample surface. The irradiance that was transmitted by the filter was ~0.06 of the total lamp irradiance in the 115–200 nm range. The lamp position and the filter combine to yield a net irradiance of ~8.4 suns in the 115–200 nm spectral range.

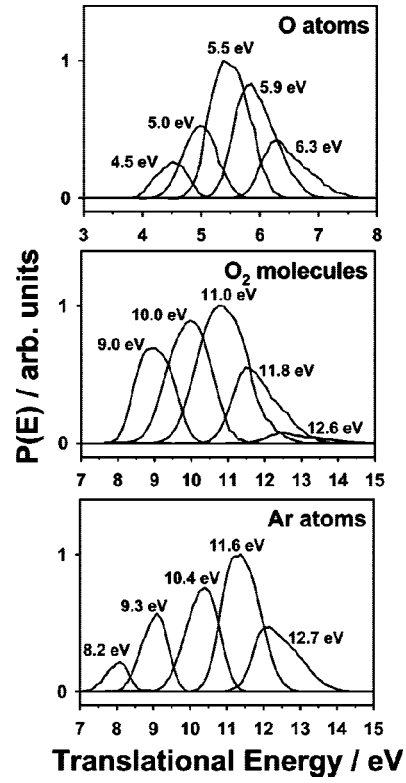

FIGURE 2. Representative translational energy distributions of hyperthermal O/O_2 and Ar beams selected with the synchronized chopper wheel.

FEP Teflon, by analogy with poly(tetrafluoroethylene) (37), is expected to absorb strongly at 161 nm, which corresponds to a transition from the highest occupied molecular orbital levels of the C–F bonds to a conduction band in the polymer. In fact, a large fraction of the VUV absorption between 115 and 200 nm occurs in this absorption band. Therefore, the photochemical effect on the sample is likely to be more dramatic than that induced by 8.4 solar equivalents in LEO, but there is insufficient information about the photochemistry and its relationship to the irradiation wavelength to draw firm conclusions.

2.3. Hyperthermal Gas–Surface Interactions. The beam-surface scattering experiments were conducted with pulsed beams, operating at a repetition rate of 2 Hz and containing hyperthermal Ar or a mixture of O and O_2. The pressure in the main scattering chamber was maintained at $\sim 1 \times 10^{-7}$ Torr throughout the experiment.

A chopper wheel was used to select narrowed portions of each overall beam pulse; the selected portions had different translational energy distributions, thus allowing the investigation of the relationship between incident translational energy and product scattering dynamics. The chopper wheel also blocked the radiation from the laser-breakdown source. Figure 2 shows representative translational energy distributions of the narrowed (chopped) O and O_2 beams used in these experiments. These distributions were derived from TOF measurements of the beam when it was directed into the detector. While representative distributions are shown in Figure 2, in the course of conducting all of the experiments reported here, the average translational energies of O and oxygen in the hyperthermal O_2 beam ranged from 4.0 to 6.5 eV and from 8.0 to 13 eV, respectively, and these species were in their ground electronic states, $O(^3P)$ and $O_2(^3\Sigma_g^-)$ (38, 39). The mole fraction of atomic oxygen in the beam varied from 50 to 80%, with higher energy beams having higher O-atom mole fractions. Hyperthermal beams of Ar (Figure 2) were also created with the laser-breakdown source and were used to investigate the CID mech-

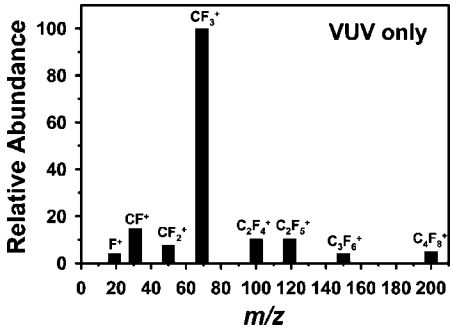

FIGURE 3. Mass spectrum of volatile products detected when an FEP Teflon surface was exposed to an unfiltered deuterium lamp 15 cm away.

anism. The average translational energies of the Ar beams used in this experiment ranged from 8.2 to 12.7 eV.

The hyperthermal beam struck the FEP Teflon target surface (placed ~92 cm from the apex of the nozzle) about 7 cm past the chopper wheel. The FEP Teflon sample was mounted on a manipulator such that the surface normal was contained in the plane of rotation of the detector. The rotation axis of the manipulator was coincident with the detector's rotation axis, and this axis passed through the sample surface. The samples were thermally isolated, and the sample mount was electrically grounded. The temperature of the sample was held at 343 K throughout the experiment, in order to reduce the adsorption of residual gases on the surface. All experiments began with pristine FEP Teflon samples, and mass-spectral data were typically collected under the following conditions: (1) VUV light alone, (2) beam-surface scattering with O/O_2 alone and then O/O_2 + VUV, and (3) beam-surface scattering with Ar alone and then Ar + VUV. In some cases, where the focus was on the combined effect of O/O_2 or Ar with VUV light, the step of beam-surface scattering with O/O_2 or Ar alone was abbreviated or skipped altogether. The possible conditions where VUV light preceded O/O_2 or Ar bombardment were not studied because they would have significantly complicated the experimental matrix and were judged to be less important in identifying combined effects than the conditions that were studied.

When the hyperthermal oxygen beams were directed at the sample, inelastically scattered products were collected at m/z = 16 (O^+) and 32 (O_2^+) and reactively scattered products that exited the surface were collected at m/z = 19 (F^+), 47 (CFO^+), 50 (CF_2^+), 66 (CF_2O^+), 69 (CF_3^+), and 85 (CF_3O^+). TOF distributions were collected for products that scattered from the surface under bombardment of the hyperthermal O/O_2 beam alone and when the surface was exposed simultaneously to VUV radiation and hyperthermal O/O_2.

When the hyperthermal Ar beams were directed at the sample, TOF distributions were collected for inelastically scattered products at m/z = 40 (Ar^+) and for collisionally dissociated products at m/z = 31 (CF^+), 50 (CF_2^+), and 69 (CF_3^+). Weak signals were detected at some higher mass-to-charge ratios indicative of additional $C_mF_n^+$ fragments. TOF distributions of volatile products that formed during simultaneous exposure to VUV radiation and hyperthermal Ar atoms were also collected.

3. RESULTS

3.1. VUV Light Alone. FEP Teflon that was exposed only to the unfiltered VUV light yielded volatile reaction products that were detected at various $C_mF_n^+$ ion fragments in the mass spectrometer (see Figure 3). There appeared to be an induction period of ~30 min after the lamp was turned on before the detected flux of $C_mF_n^+$ fragments reached a steady state. The mass-to-charge ratio with the highest intensity was m/z = 69, corresponding to CF_3^+. CF_3 may not be the most probable volatile product, however, because dissociative ionization in the electron bombardment ionizer may cause higher mass fragments to dissociatively ionize ("crack") into a variety of lower mass fragments. It is therefore difficult to identify the parent ion signals. The VUV irradiance at the sample in this experiment was very high compared to what would be experienced by a surface in LEO, and the relative peak heights in the mass spectrum might depend on the magnitude of the irradiance. Nevertheless, the fact that signals were detected at mass-to-charge ratios indicative of C_mF_n fragments suggests that C−C bond breakage in FEP Teflon can occur by a photochemical process when the incident photon energy is in the VUV region of the electromagnetic spectrum.

3.2. Ar Alone. Figure 4 shows representative TOF distributions, collected at a variety of mass-to-charge ratios, for products that scattered from an FEP Teflon surface after Ar atoms with an average translational energy of 12.7 eV collided with it. For these TOF distributions, the incidence angle, θ_i, and final angle, θ_f, were both 60° with respect to the surface normal. Time zero in these distributions corresponds to the nominal time at which the Ar beam pulse struck the surface. The observation of volatile products resulting from collisions of hyperthermal Ar atoms with a pristine FEP Teflon surface clearly indicates the occurrence of CID. The most obvious mass-to-charge ratios that could be detected were F^+, CF^+, CF_2^+, and CF_3^+. Weak signals at higher mass-to-charge ratios suggest that higher C_mF_n fragments might be dislodged from the surface by hyperthermal Ar atoms. Because of the possibility of dissociative ionization, unambiguous identification of the parent fragments is not possible. Although not shown in Figure 4, strong signals from inelastically scattered Ar atoms were observed at m/z = 40 (Ar^+) and m/z = 20 (Ar^{2+}). The resolution of the mass spectrometer (~1 amu, full width at half-maximum) allowed the weak detection of products one mass unit away from their nominal masses. This "mass leakage" is included in the TOF distributions collected at m/z = 19. Therefore, the apparent signal at this mass-to-charge ratio has components corresponding to F^+ and Ar^{2+}. The Ar^{2+} component was, in principle, assignable because its shape should match that observed at m/z = 20. However, because the signal detected at m/z = 19 (F^+) was weak, it is difficult to distinguish this signal from the overlapping signal coming from "mass leakage" from Ar^{2+} in Figure 4. Although most of the TOF signals contain a single peak at relatively short times, near 200 μs or less, the TOF distribution for m/z = 69 appears to have two components: one in the range of 100−200 μs and the other in the vicinity of 700 μs. The fast peak, at shorter arrival times, corresponds to products that leave the surface with hyperthermal translational energies and must result from Ar interactions with the surface on a time scale too short for thermal equilibrium to be reached. The slower, broader peak, at longer arrival times, corresponds to products that desorb from the surface at near-thermal energies, and their velocities may be approximated by a Maxwell−

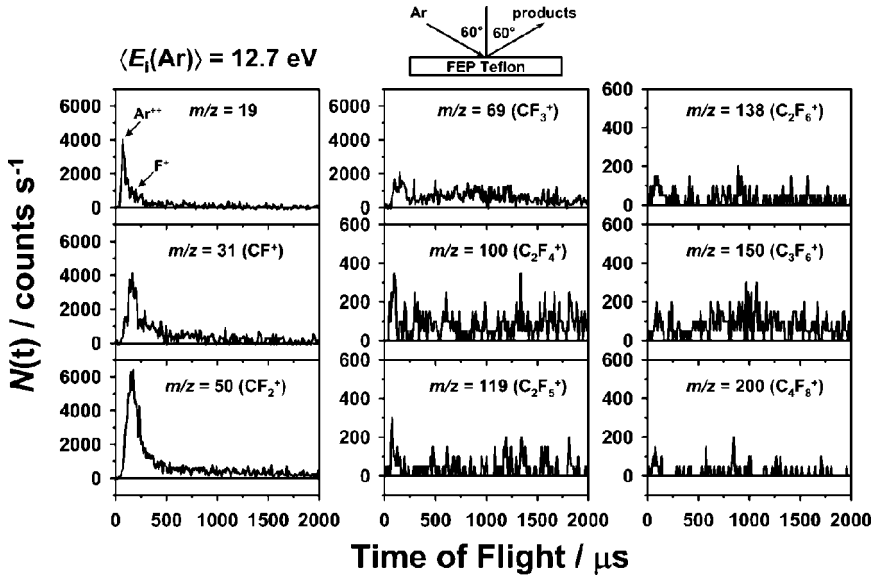

FIGURE 4. Representative TOF distributions of scattered C_mF_n fragments correlated with bombardment of a pristine FEP Teflon surface by a hyperthermal Ar beam with $\langle E_i \rangle = 12.7$ eV. The incidence and detection angles were both 60° with respect to the surface normal.

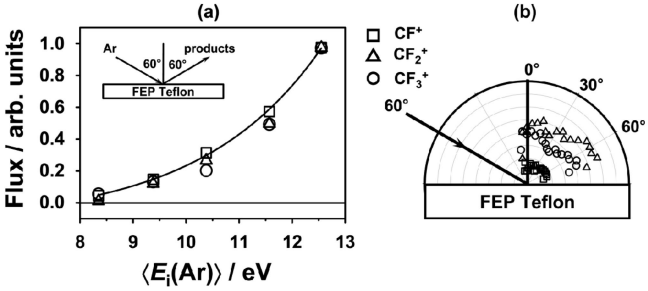

FIGURE 5. (a) Energy dependencies of CID products, detected at CF^+, CF_2^+, and CF_3^+, correlated with bombardment of a pristine FEP Teflon surface by hyperthermal Ar beams. The incidence and detection angles were both 60° with respect to the surface normal. The product flux has been normalized to the flux of the incidence Ar beam at the corresponding energy. (b) Angular distributions of CID product fluxes, detected at CF^+, CF_2^+, and CF_3^+, following exposure of a pristine FEP Teflon surface to the hyperthermal Ar beam with an incidence angle of 60°.

Boltzmann (MB) distribution at the surface temperature (343 K). This slower signal probably arises from ionizer fragmentation of much larger C_mF_n fragments that leave the surface at thermal energies. Even though only very weak signals were detected at large C_mF_n fragments (up to $m/z = 200$), ionizer fragmentation to CF_3^+ is very likely (40). Because there can be a variety of masses of the parent molecules that fragment in the ionizer to CF_3^+, the slow signal detected at $m/z = 69$ might be the result of many overlapping MB distributions, which makes it quite broad.

The TOF distributions of the products detected at CF^+, CF_2^+, and CF_3^+, produced by collisions with five energy-selected Ar beams, were converted to product flux distributions with the use of the relationship $flux(\theta_f) = \sum N(t,\theta_f)/t$. The product signals varied with the incident beam energy in part because the flux in the corresponding Ar beam varied. Therefore, product signals were normalized to the intensities of the inelastically scattered Ar atoms from the corresponding incident beams. Figure 5 shows (a) the relationship between the total flux of the product signals and the incident translational energy of the Ar atoms and (b) the angular distributions of the products detected at the three mass-to-charge ratios. The lowest energy beam, with an average translational energy of 8.2 eV, did not produce any detectable CID products. The shapes of the energy distributions (Figure 5a) for the signals detected at all three mass-to-charge ratios are the same, and the shapes of the angular distributions (Figure 5b) for the signals detected at all three mass-to-charge ratios are the same. The similar energy and angular dependencies of the products detected at all three mass-to-charge ratios suggest that a similar mechanism leads to the formation of these products. In fact, the signals detected at CF^+, CF_2^+, and CF_3^+ may come from the same radical product that exits the surface, perhaps CF_3. Ionization of CF_3 in the electron-bombardment ionizer would be expected to give the parent ion, CF_3^+, as well as the fragments, CF_2^+ and CF^+. There are numerous CF_3 groups in the FEP Teflon polymer chain, so CID to produce CF_3 may be a highly probable event.

3.3. Ar + VUV. The energy dependencies of the presumed CF_3 product detected with and without VUV light are illustrated in Figure 6 for a situation where the Ar incidence and detection (final) angles, θ_i and θ_f, respectively, were both 60° from the surface normal. A similar behavior was observed for products detected with different combinations of θ_i and θ_f (not shown). The data from the fragment detected at $m/z = 50$ (CF_2^+) were used to construct this plot because the signals were greatest at this mass-to-charge ratio. The data clearly show that the same Ar beam dissociates more products from an FEP Teflon surface that is simultaneously exposed to VUV light than from a pristine FEP Teflon surface. Above the threshold for CID production of volatile products, the ratio of the integrated product flux from the VUV-exposed FEP Teflon to that from the pristine FEP Teflon stays approximately constant at ~10, regardless of the Ar energy. The VUV light appears to alter the surface in such a way that makes the CID process more efficient, but the energy dependence of CID stays approximately the

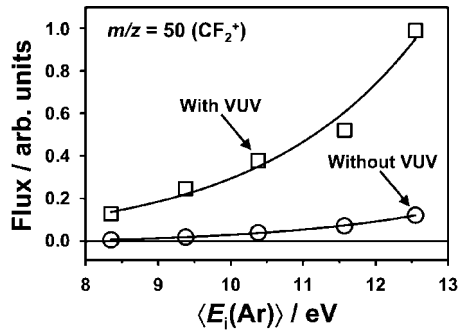

FIGURE 6. Energy dependencies of the CID product (presumed to be CF_3), detected at $m/z = 50$ (CF_2^+), correlated with the bombardment of a pristine FEP Teflon surface by hyperthermal Ar beams and simultaneous exposure of the surface to the Ar beam and to the filtered deuterium lamp placed 12.7 cm away. The incidence and detection angles were both 60° with respect to the surface normal. The product flux has been normalized to the flux of the incident Ar beam at the corresponding energy.

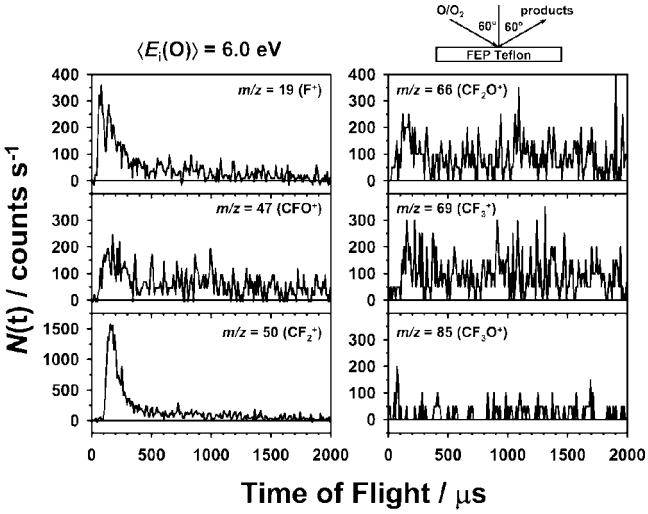

FIGURE 7. Representative TOF distributions of scattered products correlated with the bombardment of a pristine FEP Teflon surface by a hyperthermal O/O_2 beam with average translational energies of $\langle E_i(O)\rangle = 6.0$ eV and $\langle E_i(O_2)\rangle = 12.0$ eV. The incidence and detection angles were both 60° with respect to the surface normal.

same. The enhancement in the CID signal with VUV light exposure reached a steady state after an induction period of ~30 min, and then it persisted during VUV exposure and at least 3 h after the deuterium lamp had been turned off.

3.4. O/O_2 Alone. Figure 7 shows representative TOF distributions that were collected when the incidence angle, θ_i, and detection angle, θ_f, were both 60° and when the average incident O and O_2 translational energies were 6.0 and 12.0 eV, respectively. When the O/O_2 beam bombarded the surface, signals at mass-to-charge ratios indicative of O-containing products were detected at $m/z = 47$ (CFO^+) and 66 (CF_2O^+). In TOF distributions collected at $m/z = 85$ (CF_3O^+), there was a hint of a signal, but it was difficult to determine whether this very weak signal indicated a reactive product. Products detected at mass-to-charge ratios of $m/z = 19$ (F^+), 50 (CF_2^+), and 69 (CF_3^+) suggested the occurrence of CID, although dissociative ionization of reactive products may also contribute to these signals. We were unable to distinguish a signal at $m/z = 31$ (CF^+) because of interference

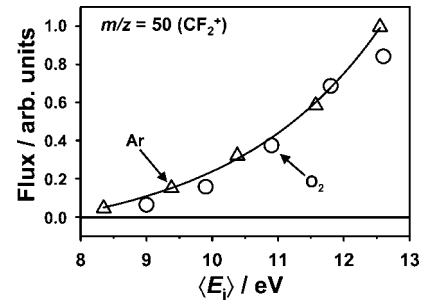

FIGURE 8. Energy dependencies of the CID product detected at $m/z = 50$ (CF_2^+), correlated with the bombardment of a pristine FEP Teflon surface by hyperthermal Ar and O/O_2 beams. The incidence energy refers to Ar and O_2. The incidence and detection angles were both 60° with respect to the surface normal. The product flux has been normalized to the flux of the corresponding Ar or O/O_2 beam at the corresponding energy.

("mass leakage") from a very high signal at $m/z = 32$, which was a result of inelastic scattering of O_2 molecules. Note that signals at all of the mass-to-charge ratios represented in Figure 7 were also observed in an earlier study that reported the mass spectra of volatile products formed when a hyperthermal O-atom beam bombarded an FEP Teflon surface (41).

Because the observed signal at $m/z = 50$ (CF_2^+) was especially strong and showed no evidence of an O-atom reaction (i.e., did not contain O), we believed this signal arose from CID caused by energetic O_2 molecules in the hyperthermal beam. We tested this supposition by studying the energy dependence of the $m/z = 50$ signal. Figure 8 compares the integrated flux of the product detected at $m/z = 50$, plotted as a function of the O_2 energy, with the dependence of a CID-induced, $m/z = 50$ flux as a function of the Ar incidence energy. The functional dependencies are exactly the same, supporting the assumption that the $m/z = 50$ signal (perhaps originating from parent CF_3 fragments that scatter from the surface) observed when the hyperthermal O/O_2 beam strikes a pristine FEP Teflon surface arises from CID caused by energetic O_2 collisions. Note that the energy dependence of the CID products released through Ar bombardment (Figure 5a) lead to the conclusion that incident particles with >8 eV of translational energy are required to promote CID at the surface. Therefore, the O atoms in the beam, even with translational energies up to 6.5 eV, do not have sufficient energy to induce a CID process.

The observation of the CFO^+ and CF_2O^+ signals indicates that O-atom reactions occur at the surface. We examined the dependence of the flux of the products detected at $m/z = 47$ (CFO^+) as a function of the translational energy of the O/O_2 beam, and the results are presented in Figure 9. The CFO^+ flux is essentially zero when the average O-atom incidence energy is 4.0 eV, and it rises monotonically as the O (or O_2) incidence energy is increased to the highest value used, 6.5 eV (or 13.0 eV). The energy dependence of the product detected at CFO^+ strongly suggests that O atoms do not react with FEP Teflon when their translational energy is ~4 eV or less. Apparently, at sufficiently high O/O_2 incidence energies (i.e., >4.0 eV for O or >8 eV for O_2), either the O atoms or O_2 molecules can react directly with the surface

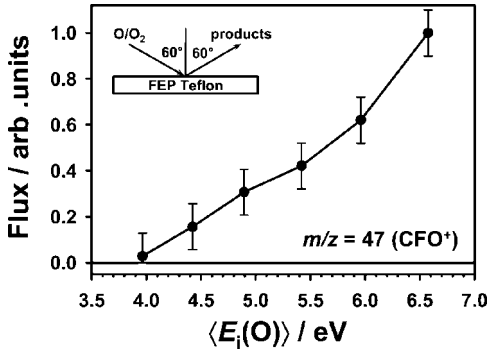

FIGURE 9. Energy dependence of the reactive, O-containing product detected at $m/z = 47$ (CFO^+), correlated with the bombardment of a pristine FEP Teflon surface by hyperthermal O/O_2 beams of various translational energies. The average incidence energy in the plot refers to O atoms in the beam; the incidence energy of the O_2 molecules is twice as high. The incidence and detection angles were both 60° with respect to the surface normal. The product flux has been normalized to the flux of the O atoms in the incidenece O/O_2 beam at the corresponding energy.

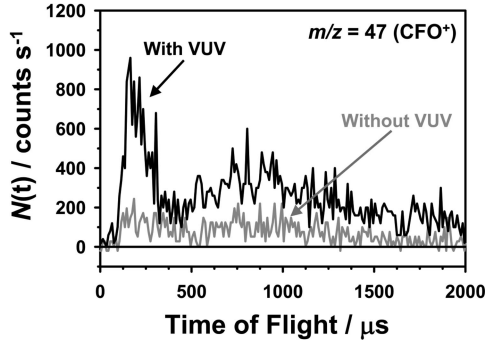

FIGURE 10. Representative TOF distributions of O-containing products, detected at $m/z = 47$ (CFO^+), correlated with bombardment of a pristine FEP Teflon surface by a hyperthermal O/O_2 beam and simultaneous exposure of the surface to the O/O_2 beam and to the filtered deuterium lamp placed 12.7 cm away. The average O and O_2 beam energies were 6.3 and 12.6 eV, respectively. The incidence and detection angles were both 60° with respect to the surface normal.

or the O_2 molecules in the beam can promote the reaction of O or O_2 by creating reactive sites through CID. If the O or O_2 reacts directly, then reactive sites would be created without the need for CID, although CID might add reactive sites.

3.5. O/O_2 + VUV. When the surface of an FEP Teflon sample was exposed simultaneously to VUV light and to the hyperthermal O/O_2 beam, the CFO^+ signal was enhanced, as seen in Figure 10. Note that the CFO^+ signal was not present with VUV light alone, so the enhancement must be the result of increased reactivity between O and/or O_2 and the surface brought about by VUV irradiation. The CID product detected at $m/z = 50$ (CF_2^+) was also enhanced in the presence of VUV light. A comparison of the dependence of the total integrated flux of the CF_2^+ signal as a function of the translational energy of the incident O_2 molecules, with and without VUV light, is shown in Figure 11. The flux was normalized to the intensities of the corresponding O_2 beams. Above the threshold for O_2-induced CID of the product, the ratio of the integrated flux from the VUV-irradiated FEP

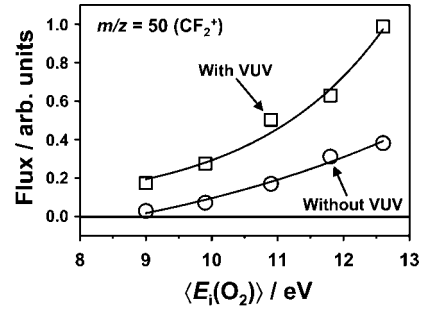

FIGURE 11. Energy dependencies of the CID product, detected at $m/z = 50$ (CF_2^+), correlated with bombardment of a pristine FEP Teflon surface to hyperthermal O/O_2 beams and with simultaneous exposure of the surface to the O/O_2 beam and to the filtered deuterium lamp placed 12.7 cm away. The incidence energy in the plot refers to O_2 molecules in the beam; the incidence energy of O is half that of O_2. The incidence and detection angles were both 60° with respect to the surface normal. The product flux has been normalized to the flux of the O_2 molecules in the incident O/O_2 beam at the corresponding energy.

Teflon to that from the pristine FEP Teflon stays approximately constant at ~2.5, regardless of the O_2 energy.

4. DISCUSSION

Individual effects of VUV light, energetic collisions, and O (and/or O_2) on FEP Teflon have been identified. VUV light clearly produces a variety of volatile radical products through photochemical bond cleavage. However, neither the product distribution nor the mass-loss rate has been quantified. Furthermore, we have not investigated the relationship between the VUV effect and VUV flux or wavelength. Energetic collisions also produce volatile radical products through CID. We have observed a threshold for the production of volatile CID products near 8 eV for the translational energy of the incident atoms or molecules. Above this threshold, the flux of products increases exponentially with incidence energy (in the range of energies studied, 8–13 eV). O atoms do not react with a pristine FEP Teflon surface up to incidence translational energies of ~4 eV. Above an energy of 4.0 eV for the O-atom component (8.0 eV for the O_2 component) of the hyperthermal O/O_2 beam, a reaction may occur, and the probability of reaction increases significantly with the collision energy of the incident atoms or molecules in the beam. The addition of VUV light enhances the likelihood of CID and O (or O_2) reactions, but we have not quantified the level of enhancement and we have not examined in detail whether the enhancement comes from initiation events, from which CID or reaction may be propagated, or if the VUV light must be present for the enhancement to be sustained.

As a model system for studying a CID mechanism, the hyperthermal interactions of Ar atoms with FEP Teflon were investigated. As described earlier for Ar-induced CID processes on oxidized polyethylene and graphite surfaces (42), the CID process on FEP Teflon likely involves the interaction of an Ar atom with a localized region of the surface. The Ar translational energy threshold observed in the earlier studies, ~8 eV, is similar to the energy threshold for CID on FEP Teflon, but because the interaction is localized, with a finite reduced mass, the c.m. collision energy may be lower by

several electron volts. Therefore, not all of the translational energy in the Ar (or O_2 molecules) would be expected to be available for bond breakage because the c.m. collision energy is dependent on the reduced mass of the system and there are many degrees of freedom at the surface where the translational energy can be dispersed.

The energy dependence of the reactive, O-containing product (see Figure 9) is consistent with the theoretical calculations of Troya and Schatz (23). They found that O atoms have extremely low reaction probabilities with C_2F_6 at c.m. collision energies below 4.5 eV and that the reaction probability increases substantially as the collision energy is increased above this value. Nevertheless, the reaction probability remained low relative to the reaction probability of O with C_2H_6 throughout the range of collision energies studied (4.5−6 eV). We observed no evidence of an O-atom reaction with a pristine FEP Teflon surface when the O-atom translational energy was 4.0 eV, and we observed an increase in the yield of reactive products as the O-atom energy was increased up to 6.5 eV. The signals were always weak, however. Although our results are consistent with the calculations of Troya and Schatz, our experiments have an ambiguity caused by the presence of O_2 in the hyperthermal beam. O_2 is much less reactive than O, but it may react at a radical site to produce a peroxy radical (25). Once such a reaction occurs, subsequent reactions may lead to the loss of a volatile O-containing product.

The formation of radical sites on or near the FEP Teflon surface may explain any combined effect that involves O atoms and either VUV light or energetic collisions. Both VUV photochemistry and CID produce volatile radical products that scatter from the surface. These processes must therefore leave radical sites on the surface. The radicals produced by VUV irradiation of FEP Teflon have been identified in an earlier study that employed electron spin resonance (25). Clearly, the simultaneous exposure of the surface to O/O_2 and VUV light enhances the yield of reactive products over that from exposure to O/O_2 alone (see Figure 10). This result is not unexpected because both O and O_2 may react at radical sites generated by the VUV light. The enhancement in the reactivity of the surface to O (or O_2) resulting from CID is perhaps less clear. Coincidentally, we observe a threshold for the production of an O-containing product (detected at CFO^+) when O_2 molecules in the beam have just enough energy to promote CID. This threshold, which corresponds to an O-atom incidence energy of 4.0 eV (see Figure 9), also corresponds to an O_2 incidence energy of 8.0 eV. In addition, we observe that the CFO^+ signal increases when the energy of O and O_2 in the beam increases. This increase in the CFO^+ signal might be the result of increasing O-atom reactivity, but it might also be the result of the increase in reactive radical sites produced by CID from O_2.

If VUV light or energetic collisions make the surface more reactive to O atoms, the resulting enhancement in reactivity may be considered to be a synergistic effect. However, the synergistic effect will only be realized in a practical situation if (1) the O-atom reactivity with the surface increases dramatically in the presence of realistic fluxes of VUV photons or energetic atoms or molecules and (2) the presence of the VUV light or energetic collisions is required to sustain the enhanced reactivity. The current set of experiments has allowed us to identify potential synergistic effects, but we have not determined if they will manifest themselves in a practical situation where FEP Teflon is exposed to an environment containing atomic oxygen with additional VUV light or energetic collisions.

The exposure of the FEP Teflon surface to VUV light increased the number of CID products resulting from Ar bombardment by an order of magnitude, and this enhancement persisted for at least 3 h after the exposure to VUV light had ceased. The VUV light apparently makes the CID process more facile. A possible explanation is that the VUV light breaks bonds and creates species on the surface with lower molecular weights, which are, in turn, easier to remove from the surface by collisions of incoming atoms or molecules. This is another combined effect that may be considered to be synergistic. However, because we do not have enough information to determine if the material removal rate with simultaneous VUV and Ar exposure is significantly greater than the sum of the material removal rates with VUV light alone and Ar atoms alone, it is unclear whether or not this newly identified synergistic effect is of practical importance.

The insights gained from the new experiments described here may help explain the erosion of FEP Teflon that has been observed on spacecraft in LEO and in ground-based test environments that contain atomic oxygen. In LEO and in many test environments, materials are exposed to VUV light. The VUV light will break bonds photochemically and create radical sites where O atoms may react. The O-atom reactions may produce volatile products, e.g., CFO, CF_2O, and CF_3O, which would carry mass away from the surface. In the residual atmosphere at LEO altitudes, N_2 molecules may have number densities that are comparable to those of O atoms (1, 2). At an altitude of 300 km, for example, the number density of N_2 is about $^1/_{10}$ that of the number density of atomic oxygen. However, at lower altitudes, ~150 km, N_2 is as abundant at atomic oxygen. N_2 molecules are almost twice as heavy as O atoms, and therefore the energy associated with collisions of N_2 with FEP Teflon is almost twice as large. Consequently, while collisions of O atoms with the ram surface of a spacecraft are equivalent to ~4.5 eV O atoms striking the surface, energetic collisions of N_2 molecules are equivalent to ~7.9 eV N_2 molecules impinging on the surface. The temperature distribution of N_2 molecules in the upper atmosphere results in a distribution of relative impact velocities that can correspond to N_2 molecules with 10 eV or greater of translational energy colliding with a ram surface. In ground-based test environments, it is possible that O_2 molecules and other neutral or ionic species with translational energies much greater than 10 eV may strike a surface simultaneously with O atoms. Therefore, in both LEO and test environments, CID from energetic collisions might break bonds and create radical sites, thus enhancing the O-atom reactivity. If VUV light is also present in the

environment, CID will be further enhanced. The enhancement of CID by VUV light would increase the material removal rate by CID and, perhaps, by the increased O-atom reactivity that could follow from the increase in the number of CID events. On the other hand, we have seen much evidence that hyperthermal O atoms can react directly with an FEP Teflon surface, and such direct reactions may dominate the erosion of the surface at moderate fluxes of VUV photons or energetic collisions. As more and more radical sites are generated by reactions with O atoms, the reaction rate would be expected to increase until a steady state is reached, where mass loss is mainly coming from the production of volatile CFO, CF_2O, or CF_3O radicals. Additional radical sites generated by VUV light or CID might only speed the approach to this steady state and, possibly, shift the steady-state erosion rate slightly. The relative importance of the various effects must depend on the details of the exposure environment. For many materials that are exposed to environments containing atomic oxygen, especially hydrocarbon-based polymers, the erosion rate is dominated by atomic oxygen reactions. However, for FEP Teflon, whose reactivity with O atoms is much lower, the erosion mechanism is complicated by the potentially important effects of additional agents, perhaps VUV light or CID, which might help initiate reactions with O atoms and increase the steady-state erosion rate.

5. CONCLUSION

Molecular beam-surface scattering experiments have probed the mechanisms by which VUV light, high-energy collisions, and atomic oxygen may act either alone or together to erode an FEP Teflon surface. The results of these experiments permit certain conclusions to be drawn about the individual and combined effects of VUV light and hyperthermal Ar or O/O_2 on FEP Teflon surfaces: (1) VUV light breaks bonds and leads to volatile C_mF_n products. (2) Energetic collisions of Ar or O_2 in the 8−13 eV range break bonds through CID and lead to volatile products. (3) The CID product flux is enhanced in the presence of VUV light, by a factor that is independent of collision energy (with the VUV wavelength and intensity used in our experiments). (4) O atoms with translational energies up to ~4 eV do not react with pristine FEP Teflon, and they likely react directly, with increasing probability, when their energies increase from this value. (5) VUV exposure and, probably, energetic collisions (from O_2 in our experiment) promote the reaction of O atoms (or O_2 molecules) with an FEP Teflon surface. Although individual and combined effects have been identified, these experiments do not elucidate the relative magnitudes of these effects, which are no doubt specific to a particular exposure environment.

Acknowledgment. This work was supported by grants from the Air Force Office of Scientific Research (Grants F49620-01-1-0335 and FA9550-07-1-0095). The authors acknowledge R. Cooper for assistance in data collection. A.L.B. is grateful for fellowships from the Zonta Foundation and the Montana Space Grant Consortium.

REFERENCES AND NOTES

(1) Champion, K. S. W.; Cole, A. E.; Kantor, A. J. In Standard and Reference Atmospheres. *Handbook of Geophysics and the Space Environment,* 4th ed.; Jursa, A. S., Ed.; Air Force Geophysics Laboratory, United States Air Force: Hauscom AFB, 1985; Chapter 14.

(2) Roble, R. G. Energetics of the Mesosphere and Thermosphere. *The Upper Mesosphere and Lower Thermosphere: A Review of Experiment and Theory*; Johnson, R. M., Killeen, T. L., Eds.; American Geophysical Union: Washington, DC, 1995; pp 1−21.

(3) Murad, E. *J. Spacecr. Rockets* **1996**, *33*, 131.

(4) Zhang, J.; Garton, D. J.; Minton, T. K. *J. Chem. Phys.* **2002**, *117*, 6239.

(5) Minton, T. K.; Garton, D. J. Dynamics of Atomic-Oxygen-Induced Polymer Degradation in Low Earth Orbit. In *Chemical Dynamics in Extreme Environments*; Dressler, R. A., Ed.; Advanced Series in Physical Chemistry; World Scientific: Singapore, 2001; Vol. 11, p 420.

(6) *Standard Solar Constant and Air Mass Zero Solar Spectral Irradiance Tables*; American Society for the Testing of Materials: West Conshohocken, PA, 2006; ASTM E490-00a.

(7) Banks, B. A. The Use of Fluoropolymers in Space Applications. In *Modern Fluoropolymers*; Schiers, J., Ed.; John Wiley: Chichester, U.K., 1997; pp 103−113.

(8) de Groh, K. K.; Smith, D. C. Investigation of Teflon FEP Embrittlement on Spacecraft in Low Earth Orbit. In *Proceedings of the 7th International Symposium on Materials in a Space Environment*, Toulouse, France, June 16−20, 1997; Guyenne, T. D., Ed.; European Space Agency: Paris, France, 1997; pp 255−265; ESA SP-399.

(9) Townsend, J. A.; Hansen, P. A.; McClendon, M. W.; de Groh, K. K.; Banks, B. A. *High Perform. Polym.* **1999**, *11*, 63.

(10) Dever, J. A.; de Groh, K. K.; Banks, B. A.; Townsend, J. A. *High Perform. Polym.* **1999**, *11*, 123.

(11) Dever, J. A.; de Groh, K. K.; Messer, R. K.; McClendon, M. W.; Viens, M. L. L.; Wang, L. L.; Gummow, J. D. *High Perform. Polym.* **2001**, *13*, S373.

(12) de Groh, K. K.; Gaier, J. R.; Hall, R. L.; Espe, M. P.; Cato, D. R.; Sutter, J. K.; Scheiman, D. A. *High Perform. Polym.* **2000**, *12*, 83.

(13) Dever, J. A.; de Groh, K. K.; Banks, B. A.; Townsend, J. A.; Barth, J. L.; Thomson, S.; Gregory, T.; Savage, W. *High Perform. Polym.* **2000**, *12*, 125.

(14) Stiegman, A. E.; Brinza, D. E.; Laue, E. G.; Anderson, M. S.; Liang, R. H. *J. Spacecr. Rockets* **1992**, *29*, 150.

(15) Koontz, S.; Leger, L.; Albyn, K.; Cross, J. *J. Spacecr. Rockets* **1990**, *27*, 346.

(16) Koontz, S. L.; Leger, L. J. ; Visentine, J. T.; Huntin, D. E.; Cross, J. B.; Hakes, C. L. An Overview of the Evaluation of Oxygen Interactions with Materials III Experiment: Space Shuttle Mission 46, July−August 1992. In *LDEF, 69 Months in Space, Third Post-Retrieval Symposium*; Proceedings of a Symposium Sponsored by the National Aeronautics and Space Administration, Washington, D.C., and the American Institute of Aeronautics and Astronautics, Washington, D.C., held in Williamsburg, VA, Nov 8−12, 1993; NASA Conference Publication 3275, Part 3; Levine, A. S., Ed.; NASA: Washington, DC, 1993; pp 869−902.

(17) Grossman, E.; Noter, Y.; Lifshitz, Y. Oxygen and VUV Irradiation of Polymers: Degradation Mechanism and Synergistic Processes. In *Proceedings of the 7th International Symposium on Materials in a Space Environment*, Toulouse, France, June 16−20, 1997; Guyenne, T. D., Ed.;European Space Agency: Paris, France, 1997; pp 217−223; ESA SP-399.

(18) Grossman, E.; Gouzman, I. *Nucl. Methods and Methods in Phys. Res. B* **2003**, *208*, 48.

(19) Yokota, K.; Ikeda, K.; Okamoto, A.; Tagawa, M. Synergistic Effects of Vacuum Ultraviolet on the Atomic-Oxygen-Induced Erosion of Fluoriniated Polymer. *Proceedings of the 10th International Symposium on Materials in a Space Environment*, Collioure, France, June 19−23, 2006; ESA SP-616 (s4).

(20) Tagawa, M.; Abe, S.; Kishida, K.; Yokota, K.; Okamoto, A. Synergistic Effect of EUV from the Laser-Sustained Oxygen Plasma in the Ground-Based Atomic Oxygen Simulation of Fluorinated Polymers. *Proceedings of the 9th International Conference on the Protection of Materials and Structures from the LEO Space Environment*, Toronto, Canada, May 20−23, 2008.

(21) Skurat, V. E.; Samsanov, P. V.; Nikiforov, A. P. *High Perform. Polym.* **2004**, *16*, 339.
(22) Gindulyte, A.; Massa, L.; Banks, B. A.; Miller, S. K. R. *J. Phys. Chem. A* **2002**, *106*, 5463.
(23) Troya, D.; Schatz, G. C. Theoretical Study of Reactions of Hyperthermal O(^{3}P) with Perfluorinated Hydrocarbons. *Proceedings of the 7th International Conference on the Protection of Materials from the Space Environment*, Toronto, Canada, May 10−13, 2004.
(24) Tasic, U.; Hein, P.; Troya, D. *J. Phys. Chem. A* **2007**, *111*, 3618.
(25) Rasoul, F. A.; Hill, D. J. T.; George, G. A.; O'Donnell, J. H. *Polym. Adv. Technol.* **1998**, *9*, 24.
(26) Rutledge, S. K.; Banks, B. A.; Kitral, M. *A Comparison of Space and Ground Based Facility Environment Effects for FEP Teflon*; NASA Technical Memorandum 1998-207918/REV1; NASA: Cleveland, OH, 1998.
(27) Weihs, B.; Van Eesbeek, M. Secondary VUV Erosion Effects on Polymers in the ATOX Atomic Oxygen Exposure Facility. *Proceedings of the 6th International Symposium on Materials in a Space Environment*, Noordwijk, The Netherlands, Sept 19−23, 1994; European Space Agency: Paris, France, 1994; pp 277−283; ESA SP-368.
(28) Van Eesbeek, M.; Levadou, F.; Milintchouk, A. A Study of FEP Behaviour in the Space Environment. *Proceedings of the 25th International Conference on Environmental Systems*, San Diego, CA, July 10−13, 1995; Society of Automotive Engineers: Warrendale, PA, 1995; Paper 951640.
(29) Dever, J. A.; McCracken, C. A. *High Perform. Polym.* **2004**, *16*, 289.
(30) Lee, Y. T.; McDonald, J. D.; LeBreton, P. R.; Herschbach, D. R. *Rev. Sci. Instrum.* **1969**, *40*, 1402.
(31) Garton, D. J.; Brunsvold, A. L.; Minton, T. K.; Troya, D.; Maiti, B.; Schatz, G. C. *J. Phys. Chem. A* **2006**, *110*, 1327.
(32) Zhang, J.; Upadhyaya, H. P.; Brunsvold, A. L.; Minton, T. K. *J. Phys. Chem. B* **2006**, *110*, 12500.
(33) Caledonia, G. E.; Krech, R. H.; Green, D. B. *AIAA J.* **1987**, *25*, 59.
(34) Minton, T. K.; Giapis, K. P.; Moore, T. A. *J. Phys. Chem. A* **1997**, *101*, 6549.
(35) Dever J. A.; Pietromica, A. J.; Stueber, T. J.; Sechkar, E. A.; Messer, R. K. *Simulated Space Vacuum Ultraviolet (VUV) Exposure Testing for Polymer Films*; NASA/TM-2002-211337; NASA: Cleveland, OH, 2002.
(36) Dever, J. A. Personal communication.
(37) Seki, K.; Tanaka, H.; Ohta, T.; Aoki, Y.; Imamura, A. *Phys. Scr.* **1990**, *41*, 167.
(38) Garton, D. J.; Minton, T. K.; Maiti, B.; Troya, D.; Schatz, G. C. *J. Chem. Phys.* **2003**, *118*, 1585.
(39) Troya, D.; Garton, D. J.; Minton, T. K.; Schatz, G. C. *J. Chem. Phys.* **2004**, *120*, 731–739. This study led to the conclusion that any O_2 in the hyperthermal O/O_2 beam must be in the ground $^3\Sigma_g^-$ state because the experiment was not able to identify an H_2O product, which was predicted by theory to be indicative of an $O_2(^1\Delta)$ reaction: $O_2(^1\Delta) + CH_4 \rightarrow H_2O + H_2CO$.
(40) NIST Chemistry WebBook, http://webbook.nist.gov/.
(41) Cazaubon, B.; Paillous, A.; Siffre, J. *J. Spacecr. Rockets* **1998**, *35*, 797.
(42) Zhang, J.; Minton, T. K. *High Perform. Polym.* **2001**, *13*, S467.

AM800015K